

# Impact of initial effective stress on the thermo-mechanical behavior of normally consolidated clay

4 Radhavi A. Samarakoon, Ph.D.

5 Post-doctoral Research Associate, Lawrence Berkeley National Laboratory, 1 Cyclotron Rd,  
6 Berkeley, CA 94720, USA; Email: rabeysir@eng.ucsd.edu

8 Isaac L. Kreitzer, B.S.

9 Graduate Research Assistant, Department of Structural Engineering, University of California  
10 San Diego, La Jolla, CA 92093-0085, USA; Email: [ikreitzer@ucsd.edu](mailto:ikreitzer@ucsd.edu)

11

12 John S. McCartney, Ph.D., P.E., F.ASCE

13 Professor and Department Chair - Department of Structural Engineering, University of California  
14 San Diego, La Jolla, CA 92093-0085, USA. mccartney@ucsd.edu (*Corresponding Author*)

15     **Abstract** This study aims to investigate the impact of initial mean effective stress on the thermo-  
16     mechanical behavior of saturated normally consolidated kaolinite clay. Specifically, a series of  
17     isotropic thermal triaxial tests in a cell equipped with image analysis for volume change tracking  
18     was performed to understand the impact of the initial mean effective stress on the drained  
19     thermal volume change response as well as the undrained shear strength before and after  
20     drained heating. Anisotropically consolidated clay specimens were recompressed isotropically to  
21     four different initial mean effective stresses corresponding to normally consolidated conditions  
22     before drained heating and undrained shearing. While contractive volumetric strains were  
23     observed during drained heating of all normally consolidated specimens, the thermal radial  
24     strains were greater than thermal axial strains due to the application of isotropic stresses after  
25     anisotropic consolidation from a slurry. The magnitude of thermal volumetric strain increased  
26     with increasing initial mean effective stress, which is a departure from expected trends from  
27     established constitutive models. A corresponding increase in undrained shear strength with both  
28     temperature and initial mean effective stress was observed. The results indicate the need for  
29     considering the impact of initial mean effective stress in geotechnical applications involving  
30     normally consolidated clay under non-isothermal conditions.

31     **Keywords:** Thermo-mechanical behavior, volume change, undrained shear strength, clay

32     **1. Introduction**

33         The thermo-mechanical behavior of clay has become an important topic of research because  
34         of increased interest in geomechanical problems involving thermal effects. As most of these  
35         geomechanical problems studied in the literature involved overconsolidated or compacted clays  
36         (i.e., cast-in-place energy piles, buffer systems for nuclear waste repositories, backfill for buried

37 electrical cables), there has not been a significant amount of attention on investigating the  
38 thermo-mechanical behavior of soft, normally consolidated clays. Recently, there has been  
39 interest in using in-situ heating to improve the engineering properties of soft clay (Abuel-Naga et  
40 al. 2006; Pothiraksanon et al. 2010; Samarakoon and McCartney 2020a, 2021; Ghaaowd and  
41 McCartney 2021; Ghaaowd et al. 2022). In-situ thermal soil improvement combines geothermal  
42 heat exchangers with vertical drains, which will be embedded in a soft clay deposit transferring  
43 heat to the surrounding soil. In addition to being used during the preconsolidation stage to  
44 expedite consolidation, the ground heat exchangers can also be used as an underground heat  
45 storage system for the building after soil improvement has been completed. When assessing  
46 thermal soil improvement methods, it is important to understand the thermo-mechanical  
47 behavior of soft clays at different initial mean effective stresses indicative of different depths in  
48 a clay layer. Within the domain of soil improvement, this study aims to investigate the role of  
49 initial effective stress on the thermo-mechanical behavior of normally consolidated clay  
50 subjected to drained heating. Specifically, the effect on undrained shear strength and volume  
51 change is considered.

52 Several researchers have investigated the thermo-mechanical response of clay (Campanella  
53 and Mitchell 1968; Hueckel and Baldi 1990; Cekerevac and Laloui 2004; Abuel-Naga et al. 2007a).  
54 Undrained heating of saturated clays leads to an increase in excess pore water pressure whereas  
55 drained heating of saturated clays results in thermal volume changes depending on the stress  
56 history of the clay. The thermal volume change of highly overconsolidated clays was observed to  
57 be expansive, elastic, and recoverable, whereas the thermal volume change of normally  
58 consolidated clays was contractive, plastic, and partly irrecoverable. Although thermal

59 volumetric strains are much smaller in comparison to volumetric strains obtained by mechanical  
60 loading, the reduction in void ratio obtained during drained heating leads to an increase in  
61 undrained shear strength for normally consolidated clays (Houston et al. 1985). The undrained  
62 shear strength of clay was observed to be dependent on temperature and different trends were  
63 seen based on the drainage conditions during heating (Houston et al. 1985; Kuntiwattanakul et  
64 al. 1995; Tanaka 1997; Abuel-Naga 2006). In general, normally consolidated clay specimens  
65 subjected to shear after undrained heating showed a decrease in undrained shear strength with  
66 temperature whereas specimens subjected to drained heating resulted in an increase in  
67 undrained shear strength with increasing temperature.

68 Constitutive models describing the thermo-mechanical behavior of clays have been  
69 developed by several researchers (Hueckel and Borsetto 1990; Cui et al. 2000; Laloui and  
70 Cekerevac 2003; Abuel-Naga et al. 2007a; Abuel-Naga et al. 2009). The thermal volume changes  
71 in these models are typically driven by changes in the apparent preconsolidation or yield stress  
72 with temperatures. As an artifact of this approach to predict thermal volume changes, these  
73 models predict the same amount of thermal volume change for normally consolidated clays,  
74 irrespective of the initial stress state or void ratio. The constitutive models were generally  
75 validated using tests conducted on initially overconsolidated clay specimens which were  
76 mechanical loaded to a normally consolidated state after drained heating to different elevated  
77 temperatures to define a relationship between the yield stress and temperature. Compression  
78 curves obtained from isothermal tests carried out at elevated temperatures showed compression  
79 curves with slopes similar to that of a compression curve at room temperature but with a shift to  
80 the left. The constitutive models developed based on these observations predicted that normally

81 consolidated clays will have the same thermal hardening response and the same amount of  
82 volume change regardless of its initial mean effective stress. While many of the models included  
83 successful validation of the volume change of a single normally consolidated clay specimen, they  
84 did not validate the model for several normally consolidated clay specimens with different initial  
85 stresses.

86 On the other hand, field tests (Bergenstahl et al. 1994), laboratory tests (Abuel-Naga et al.  
87 2007b; Uchaipichat and Khalili 2009; Ghaoowd et al. 2017) and poromechanics theories  
88 (Campanella and Mitchell 1968) show that normally consolidated, saturated clay having different  
89 initial mean effective stresses and void ratios lead to different thermal pressurization effects  
90 during undrained heating. The effect of the initial effective stress state on the thermal  
91 pressurization process leads to the hypothesis that the thermal volume change of normally  
92 consolidated clays will also be dependent on the initial mean effective stress for normally  
93 consolidated clays. However, there are limited studies in the literature where the thermal  
94 behavior of normally consolidated clays at different initial mean effective stress states were  
95 carefully investigated. In previous studies conducted by the authors on normally consolidated  
96 kaolinite specimens, it was observed that the thermal volume change and undrained shear  
97 strength was dependent on the initial mean effective stress (Samarakoon et al. 2018;  
98 Samarakoon and McCartney 2020b). Based on the observations of excess pore water pressure  
99 behavior under undrained conditions and limited experimental data on thermal volume change  
100 of normally consolidated clays, there is a need to further investigate the effect of initial mean  
101 effective stress on the thermo-mechanical behavior of normally consolidated clays. To that end,  
102 this study presents the results from an experimental investigation involving drained heating of

103 saturated normally consolidated kaolinite specimens at different initial mean effective stresses  
104 representative of different depths in a clay deposit.

105 **2. Material and Methods**

106 **2.1 Material**

107 Commercial kaolinite clay obtained from M&M Clays Inc. of McIntyre, GA was used in this  
108 study. The properties of the Georgia kaolinite clay are summarized in Table 1, including the  
109 compression indices obtained from an isotropic compression test at room temperature. The  
110 Georgia kaolinite clay is classified as CL according to the Unified Soil Classification System (USCS).

111 **2.2 Experimental set-up**

112 The laboratory tests were conducted using a modified triaxial system developed by Alsherif  
113 and McCartney (2015). A schematic of the experimental set-up is shown in Fig. 1. The triaxial  
114 system comprised of a Pyrex cell capable of withstanding high temperatures and pressures  
115 applied during testing. Heat was applied to the cell by circulating heated water from a  
116 temperature-controlled circulating bath through a stainless-steel U-shaped pipe placed inside  
117 the cell. A circulation pump able to accommodate high temperatures and pressures was used to  
118 ensure uniform mixing of cell water. Two thermocouples were placed to measure the  
119 temperature of the cell fluid and at the bottom of the specimen respectively. The thermocouple  
120 at the bottom of the specimen was included as it was presumed that greater heat losses would  
121 occur through the base pedestal of the specimen, potentially leading to lower temperatures in  
122 this region of the specimen. The temperature recorders were accurate to 0.5 °C. The cell pressure  
123 was applied using a flow pump whereas the back-pressure was controlled using a pressure panel.

124 Drainage was allowed only from the top of the specimen. Changes in the pore water pressure  
125 were monitored at the bottom of the specimen using a pore water pressure transducer.

126 Obtaining volume change measurements using outflow pipettes is challenging at elevated  
127 temperatures due to the thermal expansion of the system. Therefore, the volume change was  
128 measured using an image analysis technique in a non-contact manner. Two high resolution  
129 cameras (Nikon D7500) were used to capture the images of the specimen at specified time  
130 intervals throughout the duration of the test. For a given time, images were captured from two  
131 planes of the specimen which are perpendicular to each other. Images were converted to a binary  
132 form and the total volume of the specimen was obtained from the summation of discrete  
133 volumes associated with a series of stacked disks where the height of a single disk ( $\Delta h$ ) was one  
134 vertical pixel, and the diameter ( $d$ ) was the number of horizontal pixels (Uchaipichat et al. 2011).  
135 2D to 3D mapping for a single disk is shown in Eq. (1) and the total volume of the specimen is  
136 obtained as shown in Eq. (2) where  $n$  is the number of vertical pixels for  $\Delta h = 1$  pixel.

137  $Volume\ of\ a\ single\ disk = \pi d^2 \Delta h / 4$  (1)

138  $Total\ volume\ of\ specimen = \sum_{i=1}^n \pi d_i^2 \Delta h_i / 4$  (2)

139 An average of the volumes calculated from the two image planes was taken as the total  
140 volume of the specimen at a given time. Examples of images from the stages of processing and  
141 typical results during different stages of triaxial testing are shown in Fig. 2. Void ratios obtained  
142 from image analysis during consolidation are shown in Fig. 3, along with a comparison of void  
143 ratios obtained from pipette readings. Good agreement is seen in the trends of void ratio changes  
144 during consolidation between the measurements obtained from image analysis and pipette  
145 readings. In addition to directly calculating changes in volume using Equation (2), the results from

146 these image analyses can be used to interpret the axial and radial thermal strains, which may be  
147 useful in interpreting the thermal volume change response.

148 **2.3 Procedure**

149 The clay specimens were prepared by forming a slurry from clay and deionized water at a  
150 gravimetric water content of 130% in a commercial planetary mixer. The slurry was then poured  
151 into a hollow steel cylinder of diameter 88.9 mm with porous stones and filter paper placed on  
152 both top and bottom. The slurry was first consolidated anisotropically using a compression frame  
153 at a constant rate of 0.04 mm/min for 48 hours. Then constant vertical stresses of 26, 52, 103  
154 and 181 kPa were applied in 24 hour-long increments. At the end of this process, the clay layer  
155 was extruded from the steel cylinder and trimmed into a cylindrical specimen with a diameter of  
156 72.4 mm and height of 145 mm, making it suitable for testing in the thermal triaxial cell. The  
157 specimen was back-pressure saturated by applying cell pressure and back-pressure in stages until  
158 the Skempton's pore water pressure parameter B was at least 0.95. Then the specimen was  
159 isotropically consolidated by applying a specified mean effective stress. Four different mean  
160 effective stresses were considered in this study as 230, 260, 290 and 320 kPa respectively. While  
161 these mean effective stresses are on the high range for the thermal soil improvement application  
162 discussed above, these values were chosen to ensure that the specimens were at normally  
163 consolidated conditions at the stress states considered. It is assumed that normally consolidated  
164 clay specimens at lower mean effective stresses will also have the same behavior as past studies  
165 have shown that stress history is the most important variable in the thermo-mechanical behavior  
166 of clays (e.g., Hueckel and Borsetto 1990; Cui et al. 2000; Laloui and Cekerevac 2003; Abuel-Naga  
167 et al. 2007a; Abuel-Naga et al. 2009).

168 A total of 8 tests were conducted in this study, with each test requiring approximately 2 weeks  
169 to perform including specimen preparation. The first set of tests were at room temperature  
170 (24 °C), where 4 specimens were first isotropically consolidated to the 4 different mean effective  
171 stresses mentioned above respectively. In these tests the cell pressure was increased using ramp  
172 loading and the back pressure was maintained constant to subject the specimen to the specified  
173 effective stress. The applied isotropic stress state was maintained until the volume change of the  
174 specimen reached steady state. After reaching the end of primary consolidation, the specimens  
175 were sheared under undrained conditions. The second set of tests were conducted at the same  
176 mean effective stresses mentioned above but under elevated temperature. Specifically, after  
177 reaching the end of primary consolidation under the target mean effective stresses in the thermal  
178 triaxial cell, the specimens were subjected to drained heating where the cell temperature was  
179 increased from room temperature to 59.5 °C. After the specimens reached thermo-mechanical  
180 equilibrium, they were subjected to undrained shearing at the elevated temperature. A summary  
181 of the thermo-mechanical stress paths for the thermal triaxial tests are shown in Fig. 4.

182 **3. Results**

183 **3.1 Typical Time Series Results**

184 The change in mean effective stress, excess pore water pressure and temperature for a typical  
185 thermal triaxial test (target mean effective stress at heating = 290 kPa) is shown in Fig. 5. The  
186 mean effective stress increases during isotropic consolidation and remains constant throughout  
187 the test apart from a slight decrease observed at the onset of heating. Correspondingly, an  
188 increase in pore water pressure is also observed at the onset of heating. This is due to the  
189 relatively fast rate of increase in temperature at the beginning of the heating stage. With the

190 sudden increase in temperature and the low permeability of the clay specimen, partially drained  
191 conditions prevail at the beginning of the heating stage. As the temperature stabilizes with time  
192 and the excess pore water pressures dissipate, the mean effective stress returns to its original  
193 value. The temperature is measured at the top of the cell as well as the bottom of the specimen.  
194 Although both measurements of temperature follow similar trends, a difference of 8.6 °C is  
195 observed between the two locations during heating. This is a relatively large difference that is  
196 likely due to greater thermal losses through the base pedestal of the cell. Nonetheless, all heated  
197 tests were performed with the same conditions, so the effects of the mean effective stress could  
198 still be assessed. The cell temperature is shown in all subsequent figures as it is assumed to  
199 represent the temperatures on the top and sides of the cylindrical specimen.

200 An advantage of using the image analysis for strain measurement is that the axial and radial  
201 strains can be calculated separately in addition to the volumetric strain. As mentioned, the  
202 specimen was divided into a series of stacked disks where the height of a disk was one pixel. The  
203 diameter at a given height was the number of horizontal pixels. The diameter of the specimen at  
204 a given time was obtained using an average of diameter values obtained along the height of the  
205 specimen. The height of the specimen was obtained in a similar manner where it was discretized  
206 into vertical disks. The variations in axial and radial strains during isotropic consolidation and  
207 drained heating are shown in Fig. 6(a) for a typical thermal triaxial test performed at a target  
208 initial mean effective stress of 290 kPa. In this test, the radial strain measured during isotropic  
209 consolidation is greater than the axial strain. Furthermore, the rate of increase in strain at the  
210 beginning of consolidation is higher in the radial direction. During drained heating, the thermal  
211 strains show a similar behavior where more deformation is observed in the radial direction with

212 a smaller increase in axial strain. The radial strain can be observed to be compressive during  
213 heating followed by a slight expansion. The variation of axial and radial strains during drained  
214 heating is shown in Fig. 6(b). Similar behavior was observed for the specimens at other initial  
215 mean effective stresses.

216 The reason for the difference in axial and radial strains during heating under an isotropic  
217 stress state is likely due to the preparation of the clay specimens using anisotropic consolidation  
218 from a slurry. The kaolinite slurry was consolidated in a cylindrical mold in an oedometric stress  
219 state. The slurry was first consolidated by applying a constant strain rate and then subjected to  
220 vertical stress incrementally. As no strain was allowed in the radial direction,  $K_0$  conditions can  
221 be assumed during the specimen preparation stage. During triaxial testing however, the  
222 specimens were consolidated to a normally consolidated state under an isotropic stress state. As  
223 a result of the specimen preparation process under  $K_0$  conditions, the behavior of the specimen  
224 may be affected by stress-induced anisotropy. Most studies evaluating thermal volume change  
225 behavior were conducted using oedometers or triaxial cells and the results are typically reported  
226 as volumetric strains. However, the presence of stress-induced anisotropy may impact the  
227 deformation of the specimen when subjected to mechanical and thermal loading. Coccia and  
228 McCartney (2012) developed a new thermo-hydro-mechanical true triaxial cell which had the  
229 ability to subject soil specimens to different anisotropic stress states. Tests were conducted on  
230 cubical specimens of saturated overconsolidated Bonny silt and plastic contraction in the major  
231 stress direction and elastic expansion in the minor stress direction was observed as the initial  
232 stress anisotropy increased during heating. Similar observations were made by Shanina and  
233 McCartney (2017) for cubical specimens of unsaturated silt. To assess this, radial and axial strain

234 trends during isotropic consolidation and drained heating were investigated. While the reason  
235 for reporting thermal deformations in the literature only in terms of void ratio or volumetric  
236 strain may be the difficulty of measuring both axial and radial strains in conventional triaxial and  
237 oedometric tests. This issue was resolved in this study using image analysis for measurement of  
238 axial and radial strains.

239 Based on these observations, although the specimens were subjected to isotropic stress  
240 states in the thermal triaxial cell, the strain response of the specimens during mechanical loading  
241 and heating was anisotropic with greater radial strains than axial strains. This may be due to the  
242 specimen preparation process where the specimen was consolidated under axial loading in the  
243 vertical direction with no allowance for radial deformation. As the specimen continued to  
244 contract during drained heating, similar behavior is observed. Although the thermal strains are  
245 smaller in comparison, radial strain during drained heating is still observed to be larger than the  
246 axial strain. Hueckel and Pellegrini (1996) obtained similar results for Boom clay where plastic  
247 contractive strain was larger in the horizontal direction than in the vertical direction during  
248 heating under an isotropic stress state. The component of horizontal stress during isotropic  
249 loading is higher than that during  $K_0$  consolidation. It was speculated that the arrangement of  
250 clay microstructure during  $K_0$  compression may mainly leave space between horizontal  
251 neighboring clusters and their closure during heating will results in larger lateral thermal strains.  
252 Hattab and Fleureau (2011) experimentally investigated the orientation of kaolinite  
253 microstructure during different stages of loading using SEM picture analysis. Similar to this study,  
254 specimens were first anisotropically consolidated and a structural anisotropy with a preferred  
255 orientation of particles in the horizontal direction was observed from the SEM images. After

256 subsequent isotropic compression in a triaxial cell, a rotation of particles and a decrease in pore  
257 space was observed reflecting a tendency towards structural isotropy.

258 The variations in void ratio and temperature are shown in Fig. 6(c) for a typical test at a target  
259 initial mean effective stress of 290 kPa during mechanical consolidation and drained heating. As  
260 expected, the void ratio decreases during mechanical consolidation and a further decrease is  
261 observed during drained heating. In comparison, the change in void ratio during drained heating  
262 for a cell temperature increase of 35.5 °C is smaller than that obtained during mechanical  
263 consolidation. Care was taken to ensure that primary consolidation was completed prior to  
264 starting the heating stage. The variation in void ratio during drained heating is shown in Fig. 6(d).  
265 Similar to the radial strain, the void ratio decreases indicating compression during heating,  
266 followed by a slight expansion. The compression curve for the same test is shown in Fig. 7. During  
267 drained heating, the specimen is subjected to contractive volume change at the given target  
268 mean effective stress.

### 269 **3.2 Consolidated Undrained Shearing Results**

270 For the heated tests, once the specimens reached equilibrium during the drained heating  
271 stage, they were subjected to shear under undrained conditions. The specimens tested at room  
272 temperature were sheared under undrained conditions after primary consolidation was  
273 completed. The consolidated undrained triaxial compression test results for specimens at room  
274 temperature and after heating are shown in Fig. 8. The principal stress ratio versus axial strain,  
275 maximum principal stress difference versus axial strain and excess pore water pressure versus  
276 axial strain are shown in Figs. 8(a), 8(b), and 8(c), respectively. In the tests on heated and not  
277 heated tests, the principal stress ratios in Fig. 8(a) increase nonlinearly until reaching a peak value

278 at an axial strain of approximately 15%, at which point the maximum frictional response of the  
279 specimens is mobilized. The maximum principal stress differences in Fig. 8(b) increased  
280 nonlinearly to a maximum value at axial strains between 10 and 15%, followed by a slight  
281 softening with continued shearing. The excess pore water pressure in Fig. 8(c) was positive in all  
282 tests and increased until reaching a maximum value at axial strains ranging from 10-15%. In  
283 comparison to the tests on specimens at room temperature, an increase in the maximum  
284 principal stress difference is observed for the specimens sheared at a cell temperature of 59.5 °C  
285 for all initial mean effective stresses considered. The excess pore water pressure generated  
286 during shear was smaller at 59.5 °C for the initial mean effective stresses considered, which led  
287 to a greater mean effective stress at failure for the heated specimens. Overall, the stress-strain  
288 curves in Figure 8 correspond to those expected for normally consolidated clays for the unheated  
289 specimens and to those expected for lightly overconsolidated clays for the heated specimens.

290 The effective stress paths for the normally consolidated specimens sheared at room  
291 temperature and after heating are shown in Fig. 9(a). The maximum principal stress difference  
292 values fall onto the same peak failure envelope irrespective of their heating path. A similar  
293 observation was made in a previous study conducted by the authors where different heating  
294 paths at different initial mean effective stresses were considered (Samarakoon et al. 2018). The  
295 stress paths during consolidated undrained shearing at 24 °C are correspond to those expected  
296 for normally consolidated clays. On the other hand, for the mean effective stress states of 230,  
297 260 and 290 kPa, the stress paths correspond to a lightly overconsolidated state. This behavior is  
298 consistent with the results observed in literature where an overconsolidated behavior was  
299 observed in initially normally consolidated specimens upon further mechanical loading after

300 drained heating (Towhata et al. 1993; Sultan et al. 2002). It also conforms to the thermal  
301 hardening phenomena experienced by the soil subjected to an increase in temperature. The  
302 relationship between the maximum principal stress difference and the mean effective stress at  
303 failure for the 8 clay specimens is shown in Fig. 9(b). The markers represent the peaks of the  
304 maximum principal stress difference and the corresponding mean effective stress at failure, so  
305 the slope of the best fit line corresponds to the slope of the peak failure envelope. However, this  
306 line can be assumed to coincide with the critical state line for this clay as it coincides with the  
307 point of stress path tangency observed in the effective stress paths in Fig. 9(a).

308 **4. Analysis**

309 **4.1 Thermal volume change**

310 A comparison of the thermal strains at different initial mean effective stresses is shown in  
311 Fig. 10. The thermal volumetric strains obtained after drained heating at different initial mean  
312 effective stresses shown in Fig. 10(a) were compressive with a positive sign. The thermal  
313 volumetric strains range from 0.40% - 0.94% which are consistent with volumetric strain values  
314 reported in the literature for normally consolidated clays during drained heating for this  
315 temperature change (Hueckel and Baldi, 1990; Baldi et al. 1988; Delage et al. 2004; Cekerevac  
316 and Laloui 2004). The contractive volumetric strains after heating increased with increasing initial  
317 mean effective stress. This observation confirms that thermal volume change of normally  
318 consolidated clay is dependent on the initial mean effective stress, as hypothesized. It is also in  
319 accordance with the increasing trends in excess pore water generation with increasing initial  
320 mean effective stress reported by Abuel-Naga et al. (2007b) and Ghaaowd et al. (2017). The  
321 authors made similar observations in kaolinite specimens subjected to a drained heating cooling

cycle in a previous study (Samarakoon and McCartney 2020b). During drained heating, the thermal volumetric strain was observed to increase as the initial mean effective stress increased, which is also shown in Fig. 10(b). The results shown in Fig. 10(b) also indicate that the thermal axial strain and thermal radial strain increase slightly with the initial mean effective stress, with a greater increase in thermal axial strain than thermal radial strain with increasing initial mean effective stress. It should be noted that the radial and axial strains were calculated based on an average diameter and height of the specimen as described in Section 3.1 whereas the volumetric strains were obtained by considering the summations of volumes associated with a series of stacked disks. The ratios between axial strain and radial strain for normally consolidated specimens at different initial mean effective stresses is shown in Fig. 10(c). The ratios are less than 1 because the radial strain was greater than the axial strain. As expected, the strain observed during isotropic consolidation is higher than the strain during drained heating. An interesting observation is that the ratio between axial strain and radial strain increases with increasing initial mean effective stress. This indicates that as the initial mean effective stress increases, the strain response of the specimen is less anisotropic. The anisotropic strain response observed during drained heating may not be a result of thermal behavior of the clay but rather due to the inherent anisotropy in the specimen caused by the anisotropic consolidation process during specimen preparation. Although the specimen is mechanically loaded to a normally consolidated state prior to heating, there may still exist some degree of anisotropy in the specimen. As a result, we may continue to observe an anisotropic strain response as the specimen is subjected to thermal loading. Based on observations by both Coccia and McCartney (2012) and Shanina and McCartney (2017) the inherent anisotropy from soil preparation (static compaction in their case)

344 did not have a significant impact on the overall thermal volumetric strains but only on the strain  
345 response in different directions. The results in Fig. 10(c) indicate that the impact of the specimen  
346 anisotropy is less significant as the initial mean effective stress increases. Although the stress-  
347 induced anisotropy in the test specimens considered in this study was a result of the preparation  
348 process, the anisotropic stress state is representative of natural soil deposits in at rest conditions.  
349 Characterizing the thermal deformation of clays with inherent anisotropy can be useful in  
350 geotechnical applications involving thermal effects.

351 **4.2 Undrained shear strength**

352 Undrained shear strength values obtained for the normally consolidated specimens tested at  
353 different initial mean effective stresses are summarized in Fig. 11. Results for the specimens  
354 sheared at both room temperature as well as 59.5 °C are shown. It is assumed that the maximum  
355 principal stress difference corresponds to the undrained shear strength of the soil. A clear  
356 increase in undrained shear strength can be seen for the specimens sheared after heating. This  
357 increase in undrained shear strength can be attributed to the plastic volumetric contraction  
358 which occurred during drained heating. Like the results obtained for thermal volume change, the  
359 increase in undrained shear strength after heating is observed to increase with increasing initial  
360 mean effective stress. As described in the previous section, a higher degree of thermal volume  
361 change was observed as the initial mean effective stress increased. As a result of this plastic  
362 decrease in volume, the undrained shear strength after heating is also observed to increase with  
363 increasing initial mean effective stress.

364 These results are in contrast with a previous observation made by the authors (Samarakoon  
365 et al. 2018) where the amount of increase in undrained shear strength after drained heating was

366 smaller for specimens with greater initial mean effective stresses. However, this observation  
367 from the previous study was counterintuitive as it is expected that greater thermally induced  
368 excess pore water pressures are expected for clay with greater initial mean effective stresses  
369 (Ghaaowd et al. 2017). The authors attribute these inconsistencies to the differences in specimen  
370 preparation and the experimental procedures followed. For instance, the clay specimens in  
371 Samarakoon et al. (2018) were consolidated in a larger diameter mold during specimen  
372 preparation and quartered after extrusion to obtain four separate triaxial test specimens. In the  
373 current study, each triaxial specimen was consolidated individually in a smaller-diameter steel  
374 cylinder.

375 The results for thermal volumetric strain and the increase in undrained shear strength at  
376 different initial mean effective stresses are synthesized in Fig. 12. For the stress range considered  
377 in this study, the thermal volumetric strain and the undrained shear strength of normally  
378 consolidated kaolinite specimens is dependent on the initial mean effective stress. Based on the  
379 trends observed, the thermal volumetric strain and the corresponding increase in undrained  
380 shear strength increases with increasing initial mean effective stress. This is contrary to the  
381 existing thermo-elasto-plastic models where the same magnitude of volumetric strain is  
382 predicted for normally consolidated clays subjected to an increase in temperature irrespective of  
383 its initial mean effective stress. However, in applications involving normally consolidated clays  
384 such as improvement of soft clay deposits using in-situ heating, it is important to account for the  
385 effect of initial mean effective stress on the thermal behavior of clay. The findings from this study  
386 will enable users to strategically apply thermal soil improvement over different depths of a clay  
387 layer thus increasing the efficiency of the thermal soil improvement process.

388 **5. Conclusion**

389 This paper presents the results of an experimental study investigating the impact of initial  
390 mean effective stress on the thermo-mechanical behavior of saturated normally consolidated  
391 clay. Contrary to the existing thermo-elasto-plastic models, the thermal volumetric strain was  
392 observed to be dependent on the initial mean effective stress of the specimen. Thermal  
393 volumetric strain during drained heating was contractive and increased as the initial mean  
394 effective stress increased. Correspondingly, the undrained shear strength also increased with  
395 increasing initial mean effective stress. These findings are useful when configuring geothermal  
396 heat exchangers for soil improvement via in-situ heating where thermal soil improvement can be  
397 strategically applied over different depths of a clay layer. The specimen preparation process of  
398 anisotropic consolidation from a slurry was found to affect the strain response of the clay  
399 specimen where more deformation was observed in the radial direction during isotropic  
400 consolidation as well as drained heating. Further studies can be conducted on a broader range of  
401 soil types and stress states to better understand the trends of thermal behavior of normally  
402 consolidated clay and to incorporate the effect of initial mean effective stress into thermo-elasto-  
403 plastic constitutive models.

404 **CRediT authorship contribution statement**

405 **Radhavi Samarakoon:** Conceptualization, methodology, investigation, formal analysis,  
406 visualization, writing – original draft. **Isaac Kreitzer:** Investigation. **John McCartney:** Supervision,  
407 resources, funding acquisition, project administration, conceptualization, methodology, writing  
408 – review and editing.

409

410 **Declaration of competing interest**

411 The authors declare that they have no known competing financial interests or personal  
412 relationships that could have appeared to influence the work reported in this paper.

413 **Acknowledgements**

414 Funding from NSF grant CMMI 1941571 is appreciated. The opinions are those of the authors.

415 **References**

416 Abuel-Naga, H.M., Bergado, D.T., Chaiprakaikeow, S. (2006) "Innovative thermal technique for  
417 enhancing the performance of prefabricated vertical drain during the preloading process."

418 *Geotextiles and Geomembranes*. 24, 359-370.

419 Abuel-Naga, H.M., Bergado, D.T., Bouazza, A., Ramana, G.V. (2007a) "Volume change behaviour  
420 of saturated clays under drained heating conditions: experimental results and constitutive  
421 modeling." *Canadian Geotechnical Journal*. 44, 942-956.

422 Abuel-Naga, H.M., Bergado, D.T., Bouazza, A. (2007b) "Thermally induced volume change and  
423 excess pore water pressure of soft Bangkok clay." *Engineering Geology*. 89, 144-154.

424 Abuel-Naga, H.M., Bergado, D.T., Bouazza, A., Pender, M. (2009) "Thermomechanical model for  
425 saturated clays." *Géotechnique*. 59(3), 273-278.

426 Alsherif, N. A., McCartney, J. S. (2015). "Nonisothermal behavior of compacted silt at low degrees  
427 of saturation." *Géotechnique*. 65(9), 703-716. DOI: 10.1680/geot./14 P 049.

428 Baldi, G., Hueckel, T., Pellegrini, R. (1988). "Thermal volume changes of the mineral-water system  
429 in low-porosity clay soils." *Canadian Geotechnical Journal*. 25, 807-825.

- 430 Bergenstahl, L., Gabrielsson, A., Mulabdic, M. (1994), "Changes in soft clay caused by increase in  
431 temperature." *Proc. 13<sup>th</sup> International Conference on Soil Mechanics and Foundation*  
432 *Engineering*. New Delhi, India. Jan 5-10. 1637-1641.
- 433 Campanella, R.G., Mitchell, J.K. (1968) "Influence of temperature variations on soil behavior."  
434 *Journal of the Soil Mechanics and Foundation Division. ASCE*. 94(3), 709-734.
- 435 Cekerevac, C., Laloui, L. (2004) "Experimental study of thermal effects on the mechanical  
436 behaviour of a clay." *International Journal for Numerical and Analytical Methods in*  
437 *Geomechanics*. 28, 209-228.
- 438 Coccia, C.J.R., McCartney, J.S. (2012) "A thermo-hydro-mechanical true triaxial cell for evaluation  
439 of the impact of anisotropy on thermally-induced volume changes in soils." *ASTM*  
440 *Geotechnical Testing Journal*. 35(2), 227-237.
- 441 Cui, Y. J., Sultan, N., Delage, P. (2000). "A thermomechanical model for clays." *Canadian*  
442 *Geotechnical Journal* 37(3), 607–620.
- 443 Delage, P., Cui, Y.J., Sultan, N. (2004). "On the thermal behaviour of Boom clay." *Proceedings of*  
444 *the Eurosafe Conference*. Berlin, Germany. 1–8.
- 445 Ghaaowd, I., Takai, A., Katsumi, T., McCarntey, J.S. (2017) "Pore water pressure prediction for  
446 undrained heating of soils." *Environmental Geotechnics*. 4(2), 70-78.
- 447 Ghaaowd, I., McCartney, J.S. (2021). "Centrifuge modeling methodology for energy pile pullout  
448 from saturated soft clay." *ASTM Geotechnical Testing Journal*. 45(2), 332-354.
- 449 Ghaaowd, I., McCartney, J.S., Saboya, Jr., F. (2022). "Centrifuge modeling of temperature effects  
450 on the pullout capacity of torpedo piles in soft clay." *Soils and Rocks. Special Issue on Energy*  
451 *Piles*. 45(1), e2022000822.

- 452 Hattab, M., Fleureau, J-M. (2011). "Experimental analysis of kaolinite particle orientation during  
453 triaxial path." *International Journal for Numerical and Analytical Methods in Geomechanics*.  
454 35(8), 947-968.
- 455 Houston, S.L., Houston, W.N., Williams, N.D. (1985). "Thermo-mechanical behavior of seafloor  
456 sediments." *Journal of Geotechnical Engineering. ASCE*. 111(12), 1249-1263.
- 457 Hueckel, T., Baldi, M. (1990). "Thermoplasticity of saturated clays: Experimental constitutive  
458 study." *Journal of Geotechnical Engineering*. 116(12), 1778-1796.
- 459 Hueckel, T., Borsetto, M. (1990). "Thermoplasticity of saturated soils and shales: constitutive  
460 equations." *Journal of Geotechnical Engineering*. 116(12), 1765–1777.
- 461 Hueckel, T., Pellegrini, R. (1996). "A note on thermomechanical anisotropy of clays."  
462 *Engineering Geology*. 41, 171–180.
- 463 Kuntiwattanakul, P., Towhata, I., Ohishi, K., Seko, I. (1995). "Temperature effects on undrained  
464 shear characteristics of clay." *Soils and Foundation*. 35(1), 147-162.
- 465 Laloui, L., Cekerevac, C. (2003). "Thermo-plasticity of clays: an isotropic yield mechanism."  
466 *Computers and Geotechnics*. 30(8), 649–660.
- 467 Pothiraksanon, C., Bergado, D.T., Abuel-Naga, H.M. (2010) "Full-scale embankment consolidation  
468 test using prefabricated vertical thermal drains." *Soils and Foundations*. 50(5), 599-608.
- 469 Samarakoon, R.A., Ghaaowd, I., McCartney, J. S. (2018). "Impact of drained heating and cooling  
470 on undrained shear strength of normally consolidated clay." *Proc. 2<sup>nd</sup> International  
471 Symposium on Energy Geotechnics*. Lausanne. A. Ferrari, L. Laloui, eds., Vienna. 243-249.

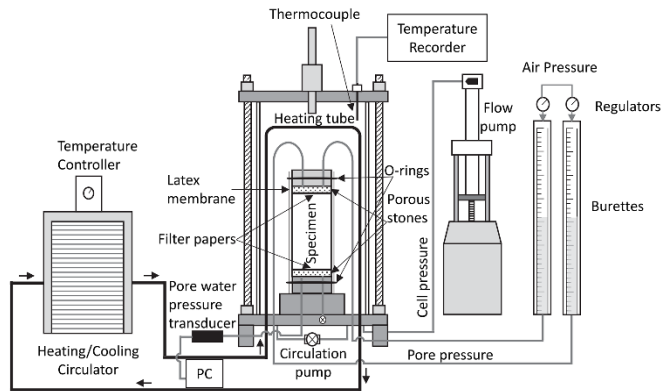
- 472 Samarakoon, R.A., McCartney, J.S. (2020a). "Analysis of thermal drains in soft clay." *Proc.*  
473 *GeoAmericas 2020: 4th PanAm Conference on Geosynthetics*. Rio de Janeiro, Brazil. Oct 26-  
474 31. 1-9.
- 475 Samarakoon, R.A., McCartney, J.S. (2020b). "Role of initial effective stress on the thermal  
476 consolidation of normally consolidated clays." *Proc. 2<sup>nd</sup> International Conference on Energy*  
477 *Geotechnics (ICEGT-2020)*. E3S Web of Conferences, Les Ulis, France. 205, 09001.
- 478 Samarakoon, R.A., McCartney, J.S. (2021). "Performance of prefabricated thermal drains in soft  
479 clay." *Geosynthetics Conference 2021*. Kansas City, MO, USA. Feb 21-24. Nicks, J. and  
480 Beauregard, M., eds. IFAI, Roseville, MI. 1-12.
- 481 Shanina, M., McCartney, J.S. (2017). "Influence of anisotropic stress states on the thermal  
482 volume change of unsaturated silt." *Soils and Foundations*. 57(2), 252-266.
- 483 Sultan, N., Delage, P., Cui, Y.J. (2002). "Temperature effects on the volume change behavior of  
484 boom clay." *Engineering Geology*. 64, 135-145.
- 485 Tanaka, N., Graham, J. Crilly, T. (1997). "Engineering behaviour of reconstituted Illitic clay at  
486 different temperatures." *Engineering Geology*. 47(4), 339-350.
- 487 Towhata, I., Kuntiwattanakul, P., Seko, I., Ohishi, K. (1993). "Volume change of clays induced by  
488 heating as observed in consolidation tests." *Soils and Foundations*. 33(4), 170-183.
- 489 Uchaipichat, A., Khalili, N. (2009). "Experimental investigation of thermo-hydro-mechanical  
490 behaviour of an unsaturated silt." *Géotechnique*. 59(4), 339-353.
- 491 Uchaipichat, A., Khalili, N., Zargarbashi, S. (2011). "A temperature controlled triaxial apparatus  
492 for testing unsaturated soils." *Geotechnical Testing Journal*. 34(5), 1-9.
- 493

494 **Table 1** Properties of Georgia kaolinite clay

Parameter	Value
Liquid Limit	47
Plasticity Index	19
Specific Gravity	2.6
Slope of VCL ( $\lambda$ )	0.09
Slope of RCL ( $\kappa$ )	0.02
USCS Classification	CL

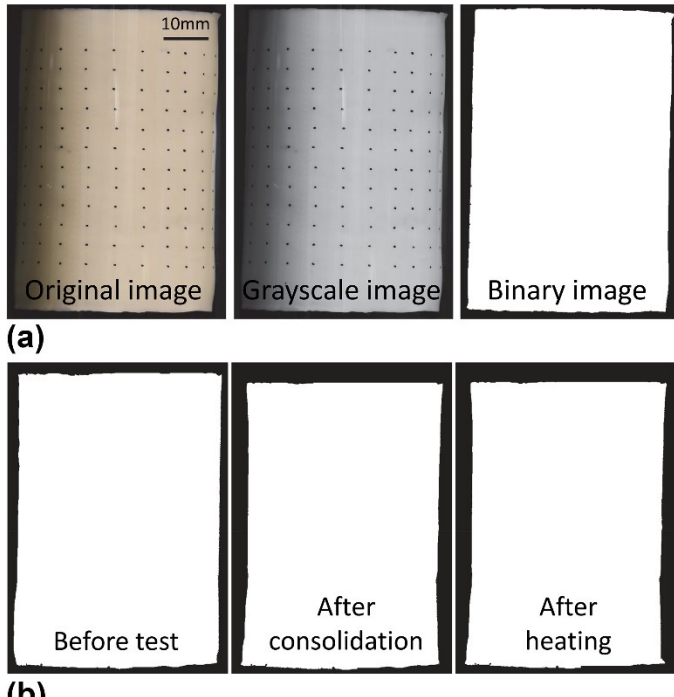
495

496



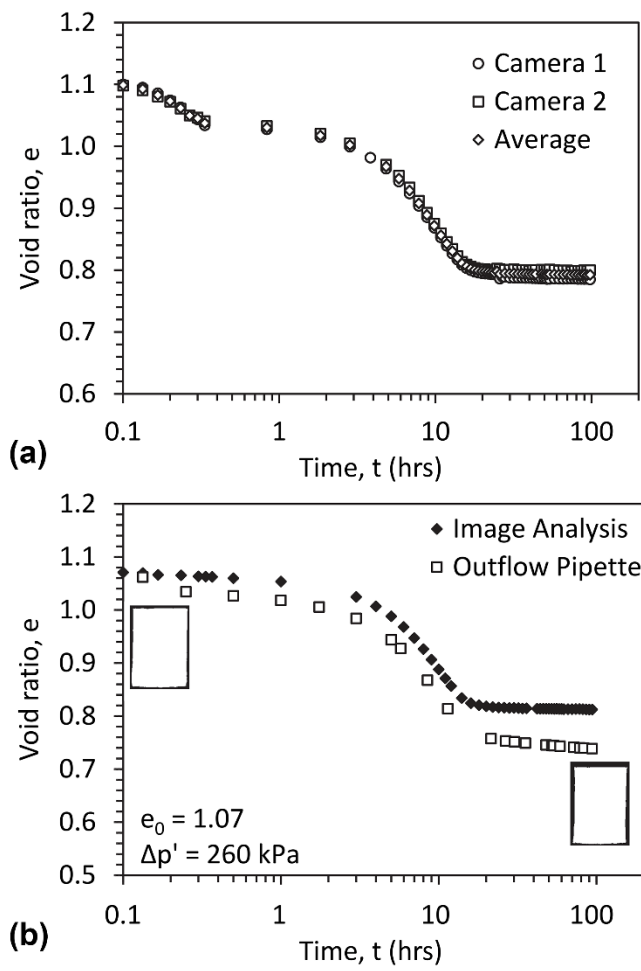
497

498 **Fig. 1.** Schematic of the thermal triaxial setup



499

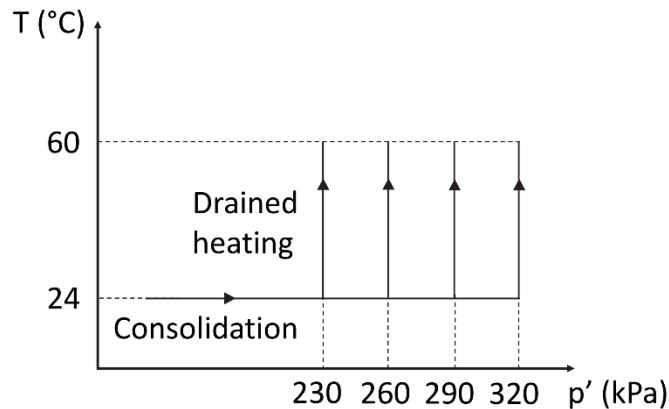
500 **Fig. 2.** Image processing: (a) Examples of images from the three stages of processing; (b) Typical  
501 results from processed images for different stages of triaxial testing



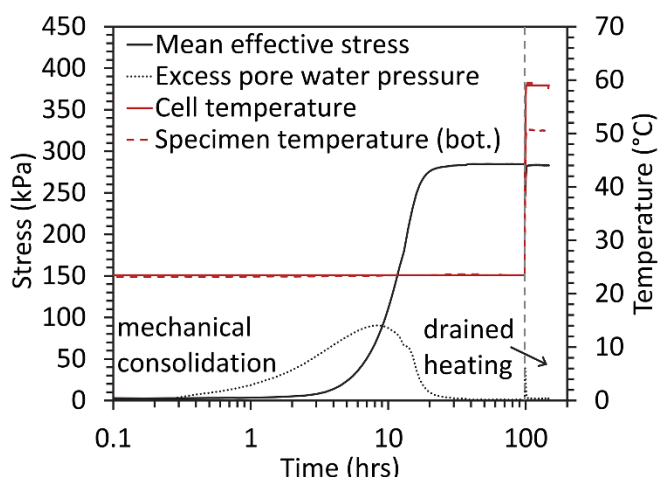
502

503 **Fig. 3.** Typical void ratio measurements: (a) Void ratio variations measured using image analysis  
 504 during consolidation; (b) Comparison of void ratios measured using image analysis and  
 505 outflow pipette readings

506

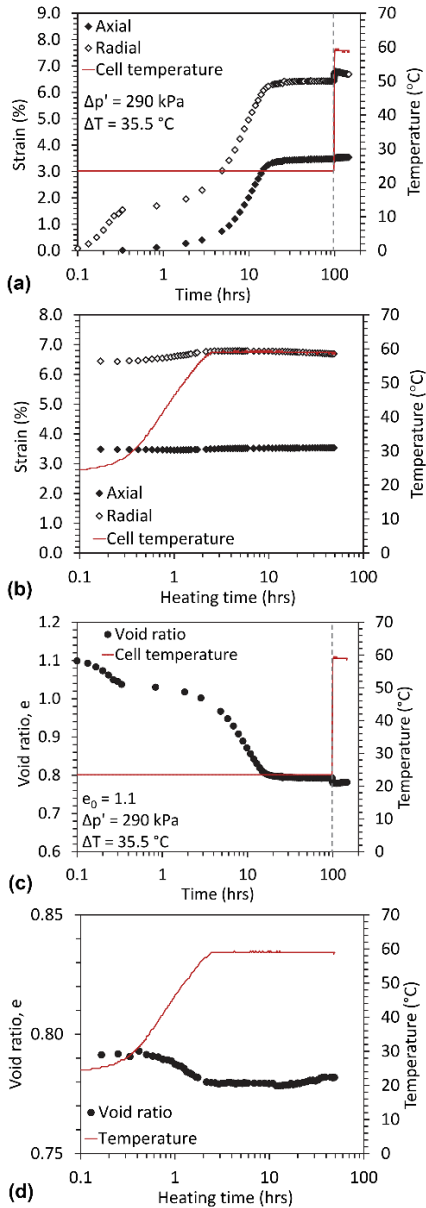


508 **Fig. 4.** Summary of the thermo-mechanical paths for the triaxial testing program



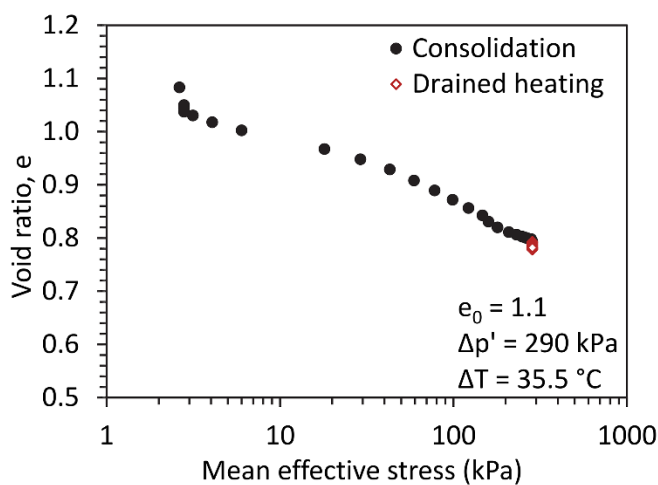
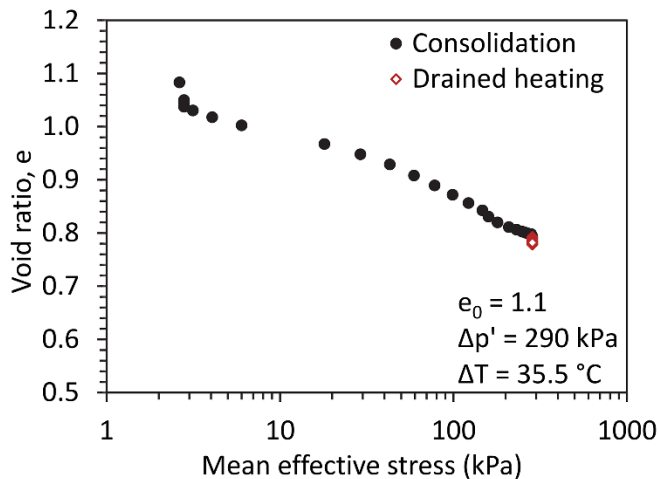
510 **Fig. 5.** Changes in mean effective stress and temperature for a typical thermal triaxial test

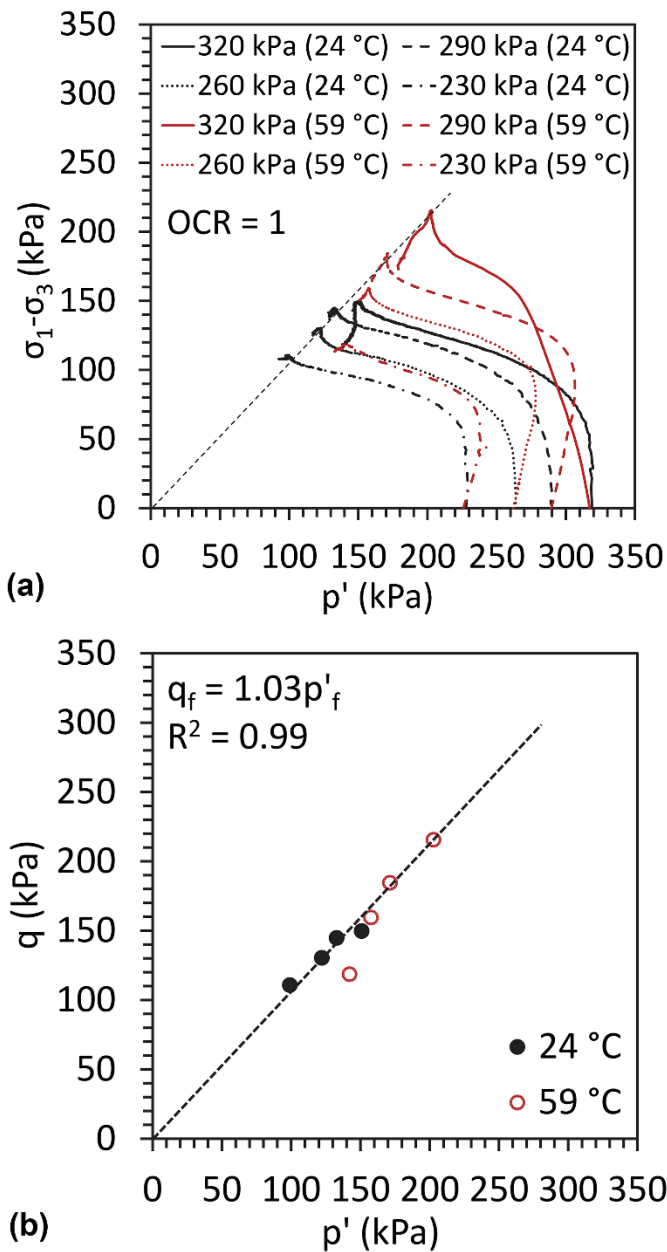
511 (target mean effective stress at heating = 290 kPa)



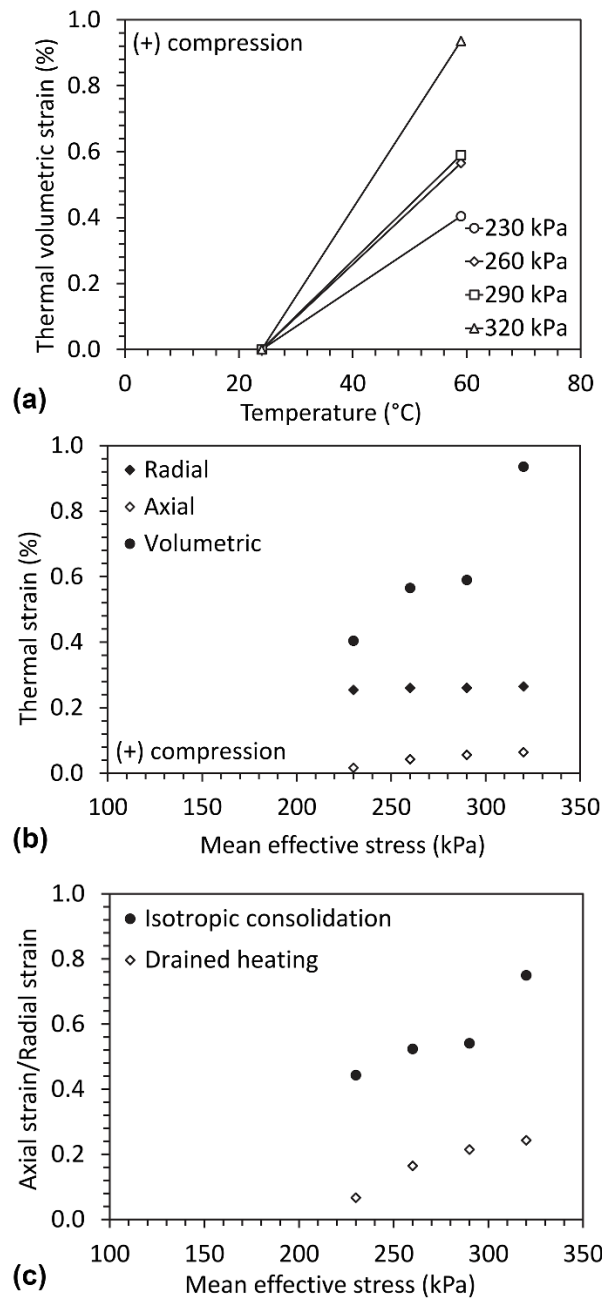
512

513 **Fig. 6.** Thermo-mechanical volume changes during different stages of a typical thermal triaxial  
 514 test at a target mean effective stress at heating = 290 kPa (Vertical gray dashed line denotes  
 515 the time when isotropic mechanical consolidation is complete and drained heating  
 516 commences): (a) Variation in axial and radial strains; (b) Variation in axial and radial strains  
 517 during drained heating; (c) Variation in void ratio; (d) Variation in void ratio during drained  
 518 heating



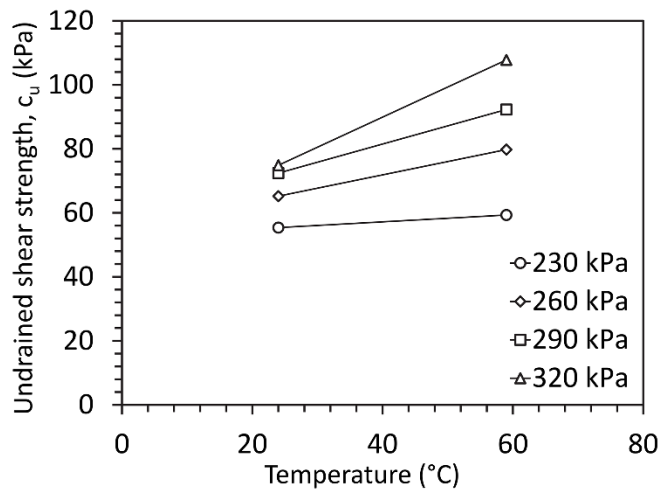


526  
527 **Fig. 9.** (a) Effective stress paths for unheated and heated normally consolidated kaolinite; (b)  
528 Relationship between maximum principal stress difference and mean effective stress at  
529 failure for normally consolidated kaolinite specimens sheared at room temperature and  
530 after heating



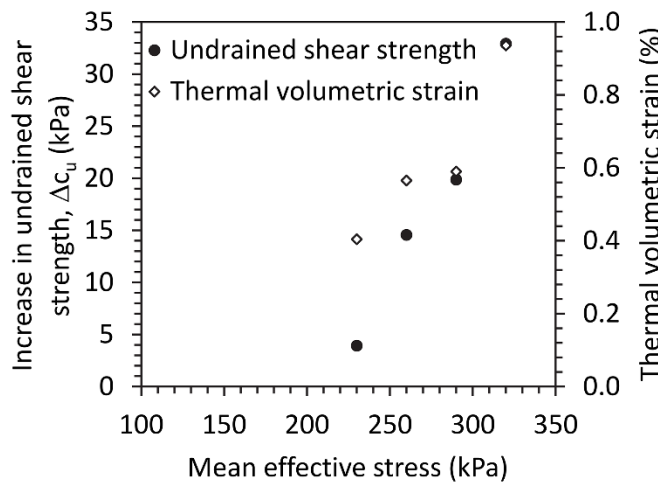
531

532 **Fig. 10.** (a) Thermal volumetric strains for normally consolidated kaolinite at different initial  
 533 mean effective stresses as a function of temperature; (b) Thermal strains for normally  
 534 consolidated kaolinite as a function of initial mean effective stress; (c) Axial to radial strain  
 535 ratios for normally consolidated kaolinite specimens at different initial mean effective  
 536 stresses



537

538 **Fig. 11.** Undrained shear strength values for unheated and heated normally consolidated  
539 kaolinite at different initial mean effective stresses



540

541 **Fig. 12.** Summary of thermal volumetric strain and increase in undrained shear strength after  
542 heating of normally consolidated kaolinite at different initial mean effective stresses